ISSN 2543-9901

JOURNAL OF CASTING & MATERIALS ENGINEERING

QUARTERLY
Vol.3 No. 2/2019

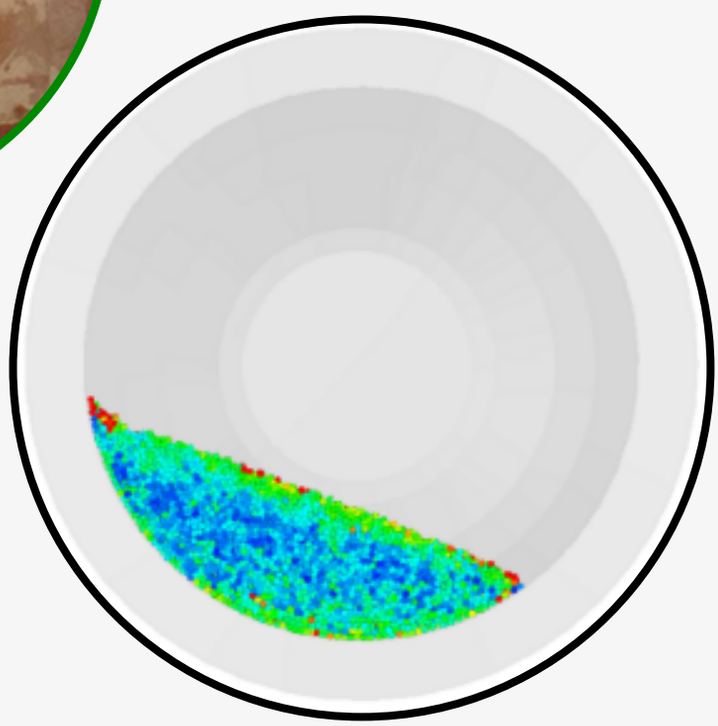

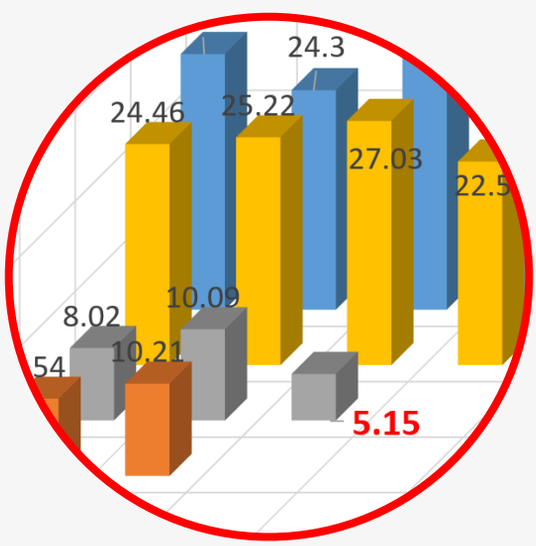

AGH UNIVERSITY OF SCIENCE AND TECHNOLOGY
FACULTY OF FOUNDRY ENGINEERING

JCME

AGH UNIVERSITY OF SCIENCE AND TECHNOLOGY PRESS KRAKOW 2019

www:
https://journals.agh.edu.pl/jcme/

AGH UNIVERSITY OF SCIENCE AND TECHNOLOGY PRESS KRAKOW 2019

Wydawnictwa AGH (AGH University of Science and Technology Press)
al. A. Mickiewicza 30, 30-059 Kraków
tel. 12 617 32 28, 12 638 40 38
e-mail: redakcja@wydawnictwoagh.pl
http://www.wydawnictwa.agh.edu.pl

Ministry of Science and Higher Education
Republic of Poland

Creating English-language versions of publications –
an assignment financed by the Ministry of Science and Higher Education
from resources allocated to science-propagating activities
according to contract 684/P-DUN/2019.

Contents

Journal of Casting & Materials Engineering Vol. 3 No. 2 (2019) 31–42
http://dx.doi.org/10.7494/jcme.2019.3.2.31

New Computer Method of Derivative Thermal Express Analysis of Cast Iron for Operational Prediction of Quality of Melts and Castings

Edvard Zakharchenko[a*], Ekaterina Sirenko[a], Alexander Goncharov[a], Alexander Bogdan[a], Andriy Burbelko[b], Magdalena Kawalec[b]

[a]Physico-Technological Institute of Metals and Alloys of the National Academy of Sciences of Ukraine, Blvd. Vernadsky 34/1, 03142 Kiev, Ukraine
[b] AGH University of Science and Technology, Faculty of Foundry Engineering, 23 Reymonta St., 30–059 Krakow, Poland
**e-mail: thermoexp.metal@gmail.com*

Received: 22 November 2018/Accepted: 27 May 2019/Published online: 30 June 2019

Abstract

This method is based on the determination of similarity criterion $\overline{Z}$ as the average temperature difference between the reference and analyzed curves in the solidification region. The purpose of this work is to describe the thermal express-analysis (TDA) device created by us and the substantiation of the reliability and sensitivity of the results of the new method, including the definition of a two-sided confidence interval using Student's *t*-test. The error of the method was determined with the Student's criterion taken into account. The high sensitivity of the method to the metallurgical prehistory of the gray and white cast iron melts was confirmed. The method has been successfully tested under laboratory and experimental-industrial conditions on induction melting cast iron. The new method uses a disposable environmentally friendly submersible steel sampler with a heat-resistant coating inside and out. The method allows for the quick adaptation to the conditions of specific foundries (especially with the frequent changes of classes and types of cast iron) due to replenishing the database of the reference samples.
The basic features of the new method are its universality, self-adaptability, speed, relative simplicity, and high sensitivity to the metallurgical prehistory of molten iron.

Keywords:

derivative thermal express-analysis, reference and analyzed cooling curve similarity criterion, gray iron, white iron, immersion sample cup

1. SELECTION AND CRITICAL ANALYSIS OF THE PROTOTYPE TDA EXPRESS-METHOD

The choice of the TDA express-method as a prototype for solving the problem of the operational prediction of the quality of cast iron[1] melts and the final properties of castings is made difficult by the lack of information about the factual development of known methods. We give a typical example from the Polish practice of casting parts from gray cast iron. Application of standard quick-cup 4011 sampler and the corresponding TDA technique at the Silesian University of Technology in Poland gave amazing results. It turned out that 55% of the silicon data, 50% of the carbon, 94% of the hardness (HB), and 86% of the tensile strength did not meet the reality [1].

Of the many TDA express-methods, a well-known method for recognizing cooling curves, described by Chinese authors [2,4–6] (hereinafter referred to as RCC) is closest to the one we offer. The prospects of this method leave no doubt because it has several important useful features; namely:

1. The direct measurement of the temperature difference of the compared melts in the liquidus-solidus interval without using regression analysis;
2. Versatility (tested for cast irons with different morphology of graphite and aluminum alloys);
3. Self-adaptability (automatically ensured by the presence of the reference cooling curves with a metallurgical history of the melts that meets the conditions of a particular foundry);
4. The speed of analysis;
5. Ease of analysis (Newtonian version TDA is used with one thermocouple and the first derivative with respect to temperature).

[1]The generic term "cast iron," which was adopted by the authors on the American model (ASM Handbook, Vol. 1A, Cast Iron Science and Technology; first printing September 2017; volume editor Dory M. Stefanescu) covers all major types of cast iron: gray iron, (flake or lamellar graphite iron), ductile iron (spheroidal graphite iron), vermicular (compacted) graphite irons, malleable irons, and special cast irons (including white irons).

However, the Chinese version of the RCC methods requires a substantial improvement (as will be shown below). According to the RCC method, a quantitative express–assessment of the quality of the cast iron melt is performed in a digital format by determining the degree of similarity of the thermal curve of the cast iron being analyzed and the group of cooling curves of the reference (reference book) cast irons with the previously measured properties accumulated in the electronic base. The quantitative determination of the degree of similarity of the cooling curves of the analyzed and reference cast irons is carried out by using special recognition criterion Ω (Omega), K [2]:

$$\Omega = \frac{|\Sigma \Delta T_i|}{n} + S \tag{1}$$

where:

$$\Delta T_i = T_i - T_i' \tag{2}$$

$$S = \left[\frac{\Sigma \left(\Delta T_i - \overline{\Delta T} \right)^2}{n-1} \right]^{0.5} \tag{3}$$

ΔT_i – the difference between measured temperature T_i on the analyzed cooling curve and reference value T'_i on the reference curve at time instant *i*;

n – the number of compared points of the compared thermal curves of cooling.

In the Chinese Formula (1), quantity $\frac{|\sum \Delta T_i|}{n}$ represents the average value of the absolute difference between the temperature of the analyzed and reference cooling curves over the entire solidification region, and *S* represents the standard deviation. The smaller the value of recognition criterion Ω, the more similar the two curves compared in the solidification area of the cast iron are. When criterion Ω is minimal or equal to zero, then the two compared curves represent the most similarity or absolute similarity to a pair. In this pair, the properties of the cast iron are considered to be the same. However, there is no one-to-one relationship between criterion Ω and the sought-after properties of the cast iron. At the same value of criterion Ω, the parameters of the properties of the analyzed cast iron differ many times. Thus, according to the experimental data of the developers themselves [2], the difference in the degree of the spheroidization of the graphite in spheroidal graphite cast iron varies from 0 to 15%, with Ω = 10 K and from 5 to 27% at Ω = 30 K. In gray cast iron with lamellar graphite, the difference in the relative content of Type A graphite varies within the limits of 20–45% at Ω = 10 K and from 37 to 80% at Ω = 20 K.

Entering variance S (standard deviation) in Formula (1) contradicts the theory of analysis and processing of the numerical measurement results and represents a gross error in the Chinese method. As is known, the numerical result provided by the measurement method is determined solely by the arithmetic average $\left(\frac{|\sum \Delta T_i|}{n} \right)$, and variance *S* characterizes only the accuracy of this numerical result [3]. The Chinese authors [2, 4–6] did not analyze the error of the RCC method at all and did not explain why some indicators of the quality of cast iron differ by almost an order of magnitude with the same Ω criterion value. Without any reasoning, the articles by the Chinese authors of the RCC method [2, 4–6] stated that the second term (*S*) in Formula (1) is supposedly necessary to take the fluctuations of the two compared cooling curves into account. However, any possible fluctuations (pulsations in magnitude) of the compared cooling curves are automatically taken into account by the RCC method when measuring the temperature difference between the curves in the liquidus solidus interval; no other cooling curve pulsations exist during the natural cooling and solidification of the melt in the sampler. Any details about the reason for introducing variance *S* in Formula (1) in the publications of the Chinese authors are missing. The Chinese expert examination [6] rightly pointed out the following disadvantages of the RCC method presented in publications [2, 4–6]: excessively high total cost, and the need for long-term costs for creating a vast reference database. Due to the erroneous input of the standard deviation index into Formula (1) (i.e., in the recognition criterion), the value of criterion Ω is increased artificially, which inevitably limits or even excludes the possibility of using this criterion to obtain a reliable result in a thermal express analysis. In addition, a significant spread in the results of the method of recognizing of curves using criterion Ω is caused by the use of an inappropriate type of sampling cup; namely, a poured sampler [7, 8].

2. EXPERIMENTAL PROCEDURE OF OUR NEW COMPUTER METHOD DERIVATIVE THERMAL EXPRESS ANALYSIS

A new similarity criterion was proposed and justified for recognizing the cooling curves (denoted as $\overline{Z}$) and the use of a submerged sampling probe, which made it possible to minimize the value of the RCC criterion within the limits of the two-sided confidence interval [9, 10].

In the more precise formula, the composition of the RCC criterion leaves the average temperature difference of the curves compared in the solidification region and eliminates standard deviation σ as an independent parameter. The structure of the specified criterion introduced a statistical characteristic; namely, the half-width of the two-sided confidence interval:

$$\delta = t_\alpha(n) \cdot \sigma / \sqrt{n} \tag{4}$$

where:

t_α – Student's *t*-criterion for a given probability (reliability) of the output and number of measurements *n*;

σ – standard deviation (mean-square error of measurements).

A trusted two-sided interval is an interval whose boundaries are functions of the sample data and that covers the true value of estimated criterion $\overline{Z}$ with a probability of at least 1-α (where 1-α is the confidence probability). In general, the calculated formula for the average criterion $\overline{Z}$ takes the following form:

$$\overline{Z} = \sum_{i=1}^{n} \left| T_{1i} - T_{2i} \right| / n \tag{5}$$

where:

T_{1i}, T_{2i} – instantaneous temperatures [°C] at the same time point of the two compared cooling curves (after the scaling transformation);
n – the number of points compared for each pair of matched curves.

For a correct comparison of the cooling curves, a scaling method is applied. This method consists of the fact that, after determining of the liquidus and solidus, the whole solidification time is divided into 1000 equal steps (where the liquidus point is considered to be 0 and the solidus point is 1000). After this, the cooling curves are compared in pairs (respectively) over the entire solidification interval.

A sampling instrument is one of the two main design units of any modern TDA device. Traditionally, samplers are made from environmentally harmful sand-resin mixtures that are manually filled with liquid iron with a spoon. To determine t_{EC}, toxic tellurium or its compounds (tellurides) are introduced into the sampler.

The following serious drawbacks of the poured type of the sand sampling cup are indicated [7, 8]:

- temperature loss of at least 50 K associated with manual transfer of the melt-spoon to the sampler position;
- changeability of filling volume;
- oxidation of the jet of iron and capture of air;
- increased heat radiation of the open surface of the molten iron in the sampler;
- uneven sample cooling.

A common drawback of poured samplers is the instability of their measurements and the insufficient resolution of their cooling curves [11, 12].

In view of the above, the traditional methods of TDA need further significant improvement (including in the design of the sampler).

Let us consider the constructive scheme of our submersible sampler as compared to other types of samplers.

A typical modern device of TDA consists of two main units:

- a sampling cup;
- a system for accumulating and processing data.

The thermocouple is pre-inserted into the cavity of the sampler. Currently, the vast majority of these types of samplers are made of sand-resin mixtures of hot curing, which are manually filled with liquid iron with a spoon. The material and design of the sampler significantly affect the shape of the thermal curve of cooling.

If formed in a good quality sampler, the latter must meet the following general requirements [11–13]:

- be continuously smooth;
- have clear bending points;
- have a straight section of a sufficient length;
- have a large slope in the liquid phase and solid phase segments;
- the temperature error should be as small as possible.

Due to the toxicity of the resins used as fasteners in the manufacture of sand-resin samplers, the latter are carcinogenic to humans and harmful to the environment at all stages of their life cycle irrespective of their design: production, use, processing, and storage in landfills. Thermocouples of the K type are usually used as thermocouples for the express-analysis of cast iron. For short-term use, these thermocouples give reliable readings at temperatures up to 1420°C. Thermocouples are protected with tips made of transparent quartz glass or a ceramic one- or two-channel tube ("straw").

The volume of the sampler has a significant influence on the determination of the carbon equivalent value and the Si content in the cast irons due to the influence of the sampler volume on the cooling rate of the sample and its structure (a decrease in volume increases the tendency towards cementite formation). The position of the hot junction of the thermocouple also affects the accuracy of the determination of CEL and Si due to the difference in the temperature gradients in the liquid iron. With a decrease in the volume of the cup, the rate of cooling the cast iron sample increases, which causes a deterioration in the shape and resolution of the thermal curve and makes it difficult to measure the parameters of the quality of the cast iron.

Our developed version of a disposable immersion steel thin-walled sampler with a refractory coating inside and outside and a disposable thermocouple bag is shown in Figure 1.

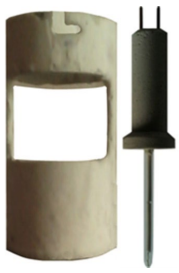

Fig. 1. Immersion steel thin-walled sampler with refractory coating inside and outside as well as disposable thermocouple bag

In accordance with the requirements for the metrological and frequency characteristics of the secondary measuring transducers for the experimental installation, a WAD-AIK--BUS four-channel analog-digital conversion module from AKON (Kiev) was chosen. This module provides reliable recording and writing down of the thermal curves for cooling metal alloys with an error in measuring thermocouple signals that are not more than 0.3 K.

The instrument part of the experimental setup includes seven basic elements (Fig. 2).

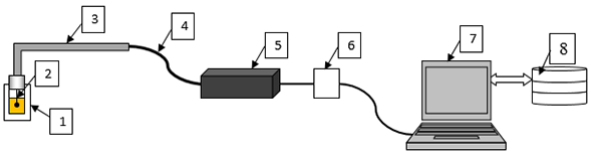

Fig. 2. Instrument part of experimental setup includes seven basic elements: 1. Calibrated probe with double-sided refractory coating; 2. Primary K-type thermoelectric measuring transducer; 3. Thermal connector with rod; 4. Connecting shielded cable for signal transmission to secondary measuring transducer; 5. WAD-AIK-BUS secondary measuring transducer; 6. Module for converting RS485/USB interface; 7. Personal computer with Project_TE software; 8. Database

In general, the algorithm of the system works as follows. The thermoelectric bag is installed in the thermocouple according to the marking on the thermocouple poles. A calibrated probe with a refractory coating is fixed on the thermo-connector of the rod. The operator immerses the probe into the melt of the cast iron so that the liquid metal fills its volume, while the thermocouple is immersed in the melt inside the probe. After filling with a melt, the probe is removed from the melt and installed with a rod into a special heat-insulating holder for cooling at rest. The secondary measuring transducer digitizes the values of the junction temperature of the thermoelectric transducer at a frequency of 10 Hz. These values are recorded on a PC in the form of two-dimensional time arrays through the procedure of question with the Project_TE program. The program processes the thermal curves of the cooling (arrays) and writes them to the database installed on the PC. The recorded reference curves as well as their corresponding chemical compositions and physical-mechanical properties are used to identify unknown controlled samples of the cast iron.

The software for the derivational thermal express analysis system includes the Project_TE control program as well as a database of the reference cooling curves, composition, and properties of the alloys ("thermoex.mdb") implemented in the MS Access database. The block diagram of the Project_TE control program action algorithm is shown in Figure 3.

The Project_TE control program is designed for the following:

- Cyclic questioning of the secondary transmitter through the RS-485 serial interface and recording the temporal cooling curves in two-dimensional data arrays;
- Determining the characteristic regions and points on the cooling curves (the solidus and liquidus temperatures as well as the primary and eutectic crystallization) using the extremums (maximum or minimum) of the first derivatives of the cooling curves;
- Transformations (scaling) of new two-dimensional arrays into arrays with a scaled time scale containing a fixed number of temperature values (1000);
- Recording the obtained cooling curves (data arrays) in the thermoex.mdb database;
- Comparing the measured cooling curve of an unknown alloy with the reference curves through the development of an algorithm for examining the reference curves, calculating the criteria for convergence, and determining the curve with the lowest criterion value;
- The formation and output of a report on the results of the analysis (on screen and printed).

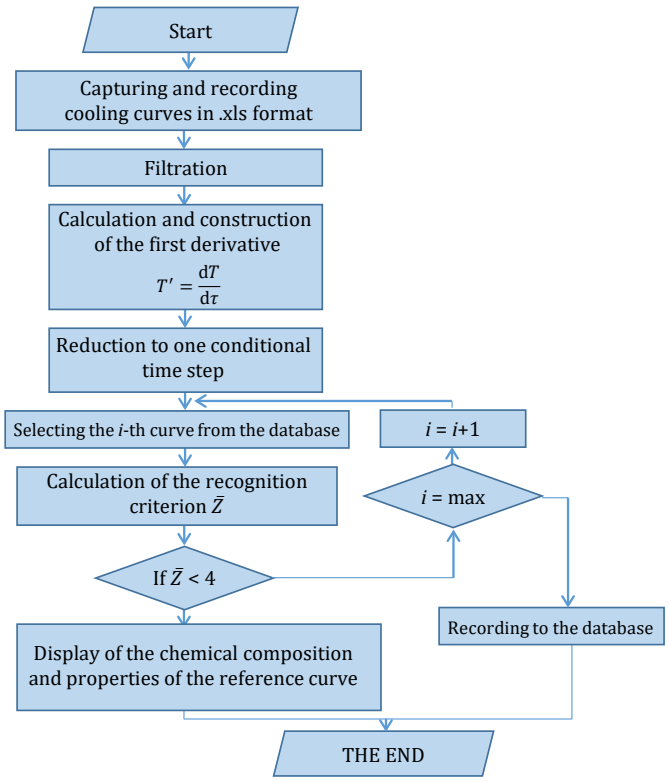

Fig. 3. Successive stages of algorithm for thermal curve processing

The experimental–industrial test of the installation of an advanced derivational thermal express-analysis of the quality of the liquid iron in an induction medium-frequency furnace (160 kg) is shown in Figure 4. The pilot-industrial test of the installation applied to a transport-melt ladle is shown in Figure 5.

Fig. 4. Experimental-industrial test of installation of advanced derivational thermal express analysis of quality of liquid iron in induction medium-frequency furnace (160 kg)

Fig. 5. Pilot-industrial test of installation of advanced derivatized thermal express analysis of quality of liquid iron as applied to transport-melt ladle

3. EXPERIMENTAL VERIFICATION OF SENSITIVITY OF TDA METHOD TO MELTS OF PARTLY AND WHITE CAST IRONS (MOTTLED IRONS)

Below are the results of the control experiments to test the sensitivity of the $\overline{Z}$ similarity criterion to hypoeutectic gray and white cast irons with different metallurgical prehistories and microstructures.

The quality control of the white iron melts using the $\overline{Z}$ criterion is relevant due to the fact that ledeburite formation (partial or full) is among the most common and expensive types of rejects of gray iron castings.

A quantitative and qualitative analysis of the microstructure of the gray and white iron samples was performed at AGH University of Science and Technology's Faculty of Foundry Engineering. The designations of the samples are 1, 2, 3, 4, 5, and 6. The samples for the preparation of the metallographic specimen were filled with acrylic resin for automatic processing.

The samples were prepared using a RotoPol-1 metallographic grinding and polishing machine using a Struers' Roto For-11 shoulder as well as special grinding and polishing materials. The samples were preliminarily polished on 80-, 120-, and 220-grit discs for five minutes. After this, fine grinding was carried out on disks with grit sizes of 600, 1200, 2000, and 4000 (also for five minutes). During the grinding, the samples and tools were cooled with water. After this preparation, the surface was polished on a MD Piano disc with a polishing cloth using a diamond suspension of 3-µm grit with the addition of DP-Lubricant and BLUE lubricant until a satisfactory visual effect was achieved.

In the course of the study, six samples of liquid iron were taken. In the laboratory smelting for Samples 1 and 2, gray cast iron was used with the following chemical composition [% mass]: 3.28 C, 2.1 Si, 0.8 Mn, and a melt mass of 2.1 kg. The filling temperature of the first sample was 1400°C. After holding the metal at 1350°C for ten minutes, the second sample was taken at a filling temperature of 1400°C. The cooling curves and their first derivatives are shown in Figure 6.

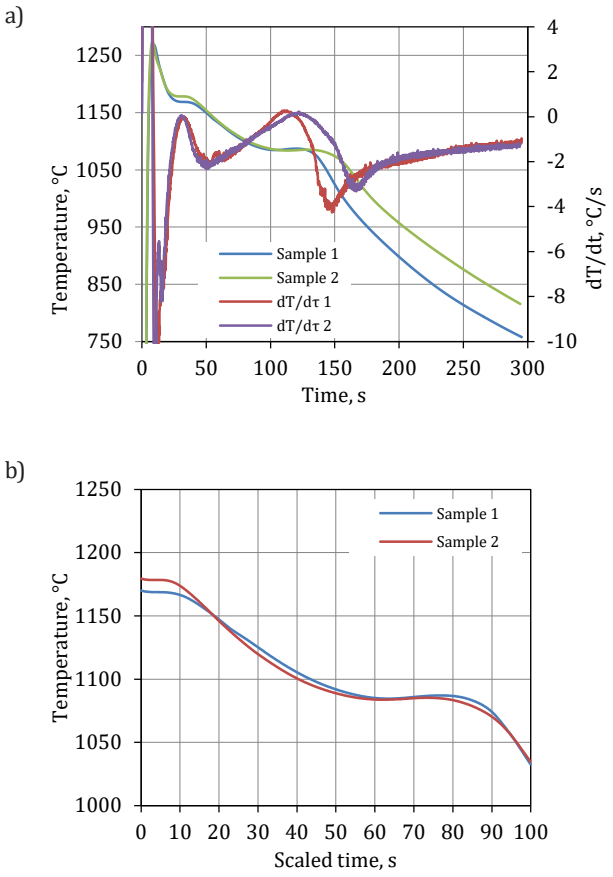

Fig. 6. Measured cooling curves and their first derivatives (a) and scaled cooling curves (b) – Samples 1 and 2

For Samples 3 and 4, cast iron of the same chemical composition was used as in Samples 1 and 2 in an amount of 1.700 kg with the addition of steel of the following chemical composition: 0.18 C, 0.8 Si, 0.5 Mn, 0.25 Cr in the amount of 0.100 kg and ferrosilicium FeSi 75 in the amount of 0.020 kg. The temperature of the third sample was 1400°C.

After holding the metal at 1330°C for 12 minutes, the fourth metal sample was taken at a temperature of 1410°C. The corresponding cooling curves and their first derivatives are shown in Figure 7.

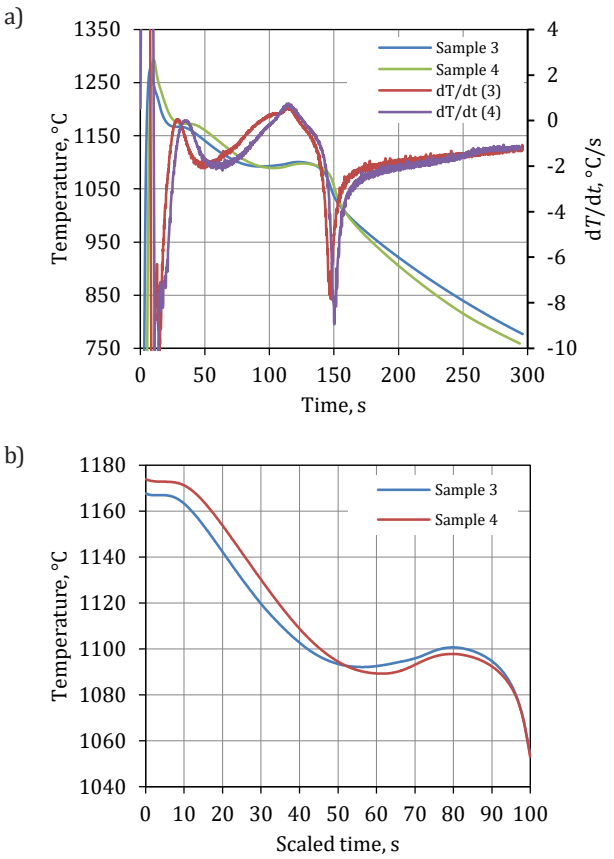

Fig. 7. Measured cooling curves and their first derivatives (a) and scaled cooling curves (b) – Samples 3 and 4

For Samples 5 and 6, cast iron of the same chemical composition as in Samples 1 and 2 in an amount of 1.680 kg with the addition of 0.200 kg of steel (0.18 C, 0.8 Si, 0.5 Mn, 0.25 Cr). The fifth sample was selected at a temperature of 1400°C (the metal was then heated to a temperature of 1410°C). The holding of the metal in the furnace was ten minutes at 1330°C, after which a sixth sample was taken at a filling temperature of 1400°C. The corresponding cooling curves and their first derivatives are shown in Figure 8.

After scaling these cooling curves, the $\overline{Z}$ criterion was calculated for all pairs of samples by comparing the curves pairwise. These results are shown in Figure 9.

As can be seen in Figure 9, the smallest values of the criterion were in the pairs of Samples 1 and 2 ($\overline{Z}$ = 3.53 K), 3 and 4 ($\overline{Z}$ = 5.15 K), and 5 and 6 ($\overline{Z}$ = 6.14 K).

Micrographs were taken on a Leica MEF4M light metallographic microscope (LM) with a Leica DFC290 camera. To quantify the microstructure, specialized Leica Q Win software was used. The actual magnification of the micrographs is represented by markers located in the micrograph field. The analysis was performed both on the non-etched thin sections (to assess the shape and placement of graphite precipitates) and after etching with Nital or Stead's reagent.

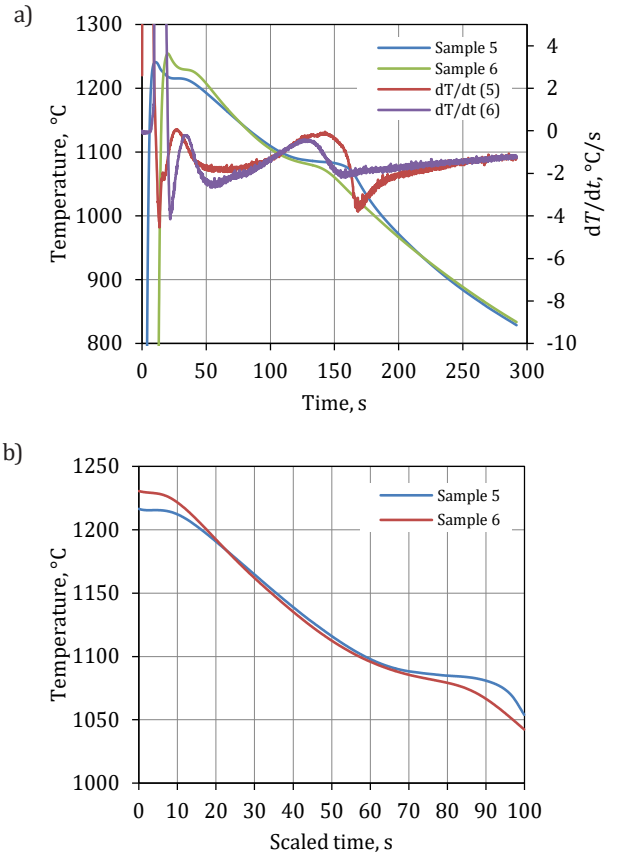

Fig. 8. Measured cooling curves and their first derivatives (a) and scaled cooling curves (b) – Samples 5 and 6

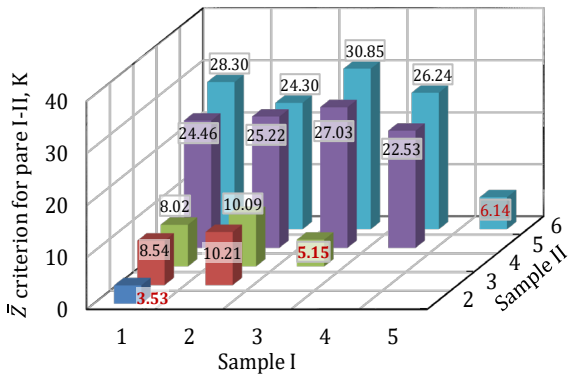

Fig. 9. Results of calculated criterion $\overline{Z}$ (K) for all pairs of samples

During the course of the analysis, a classification of the types of eutectic graphite extraction was prepared and a series of measurements of the linear parameters of these emissions was performed. Based on the images of the microstructure after etching with Stead's reagent in the samples, the number of eutectic grains was determined where possible. Based on the results of etching with Nital, the evaluation of the microstructure of the metal matrix was carried out, chill iron was detected, and the components of the microstructure of the substrate were evaluated.

The results of the analysis of the microstructure of samples using an LM microscope are presented in the form of an "atlas of the microstructures" in Figures 10–17.

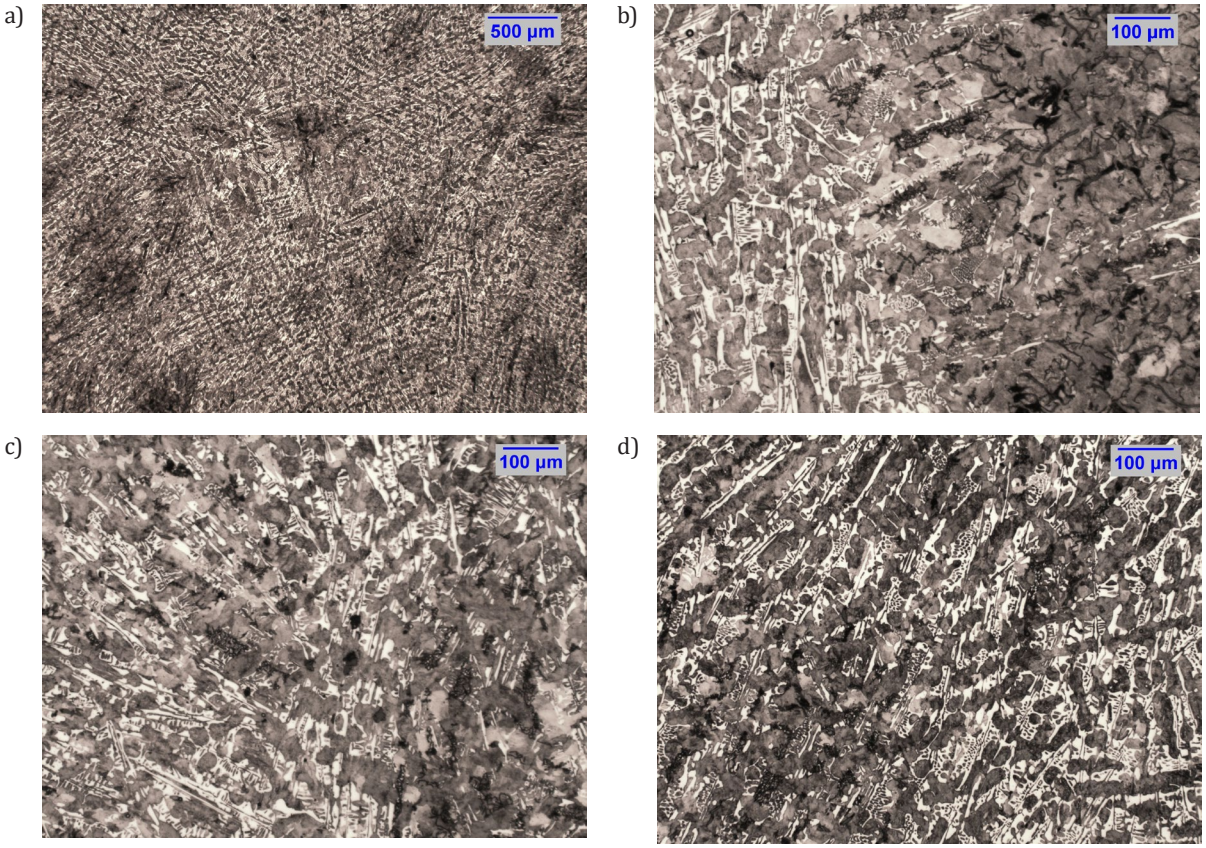

Fig. 10. Microstructure of Sample 1 etched with Nital: a) area 1, magn. 25×; b) area 2, magn. 100×; c) area 3, magn. 100×; d) area 4, magn. 100×

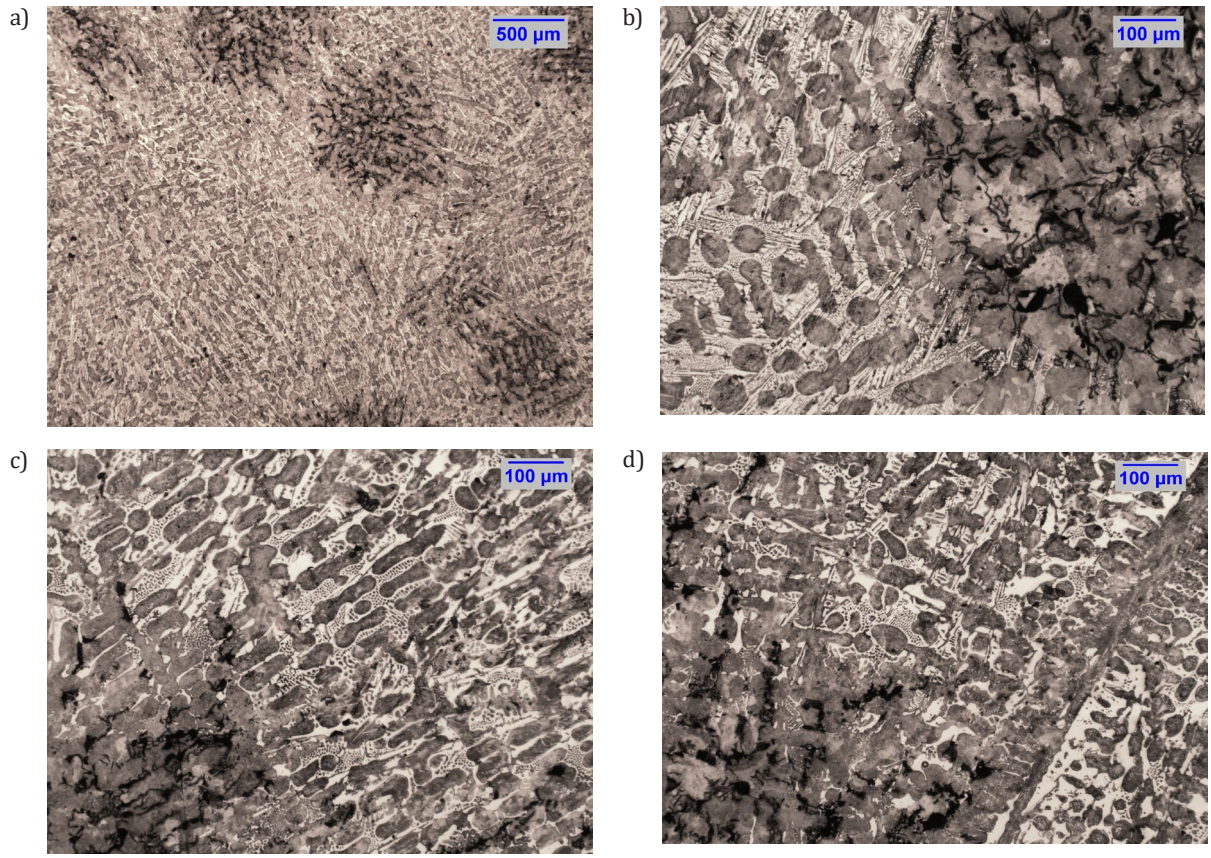

Fig. 11. Microstructure of Sample 2 etched with Nital: a) area 1, magn. 25×; b) area 2, magn. 100×; c) area 3, magn. 100×; d) area 4, magn. 100×

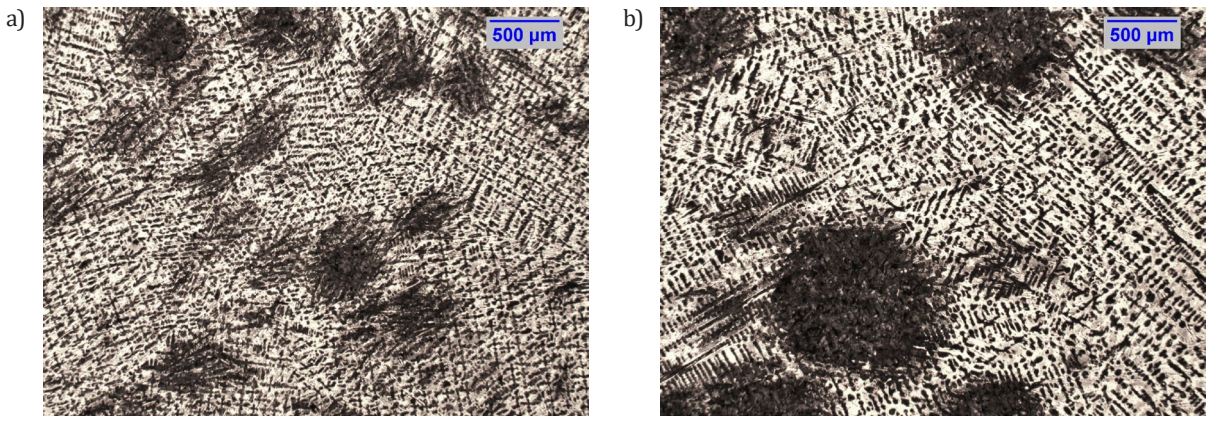

Fig. 12. Microstructure (area 5) of: a) Samples 1 and b) Sample 2 etched with Stead's reagent (magn. 25×)

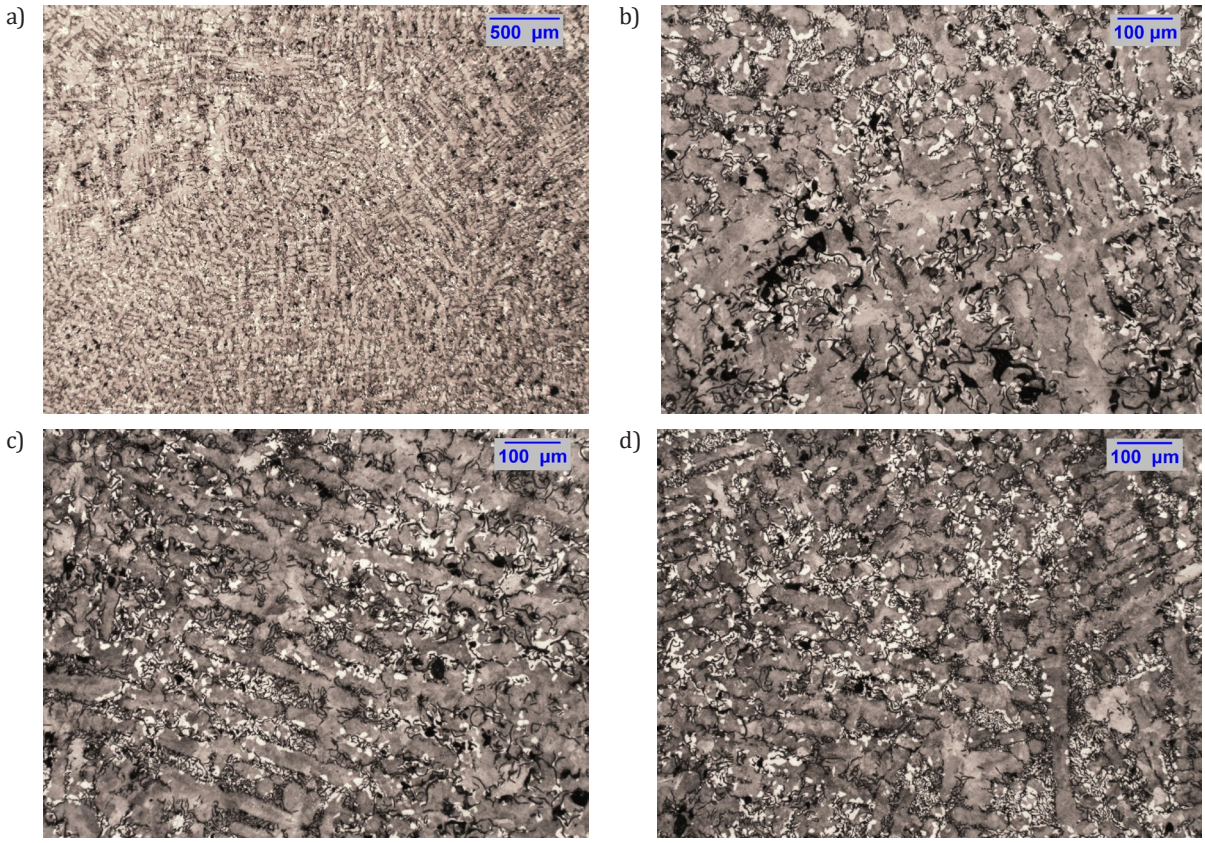

Fig. 13. Microstructure of Sample 3 etched with Nital: a) area 1, magn. 25×; b) area 2, magn. 100×; c) area 3, magn. 100×; d) area 4, magn. 100×

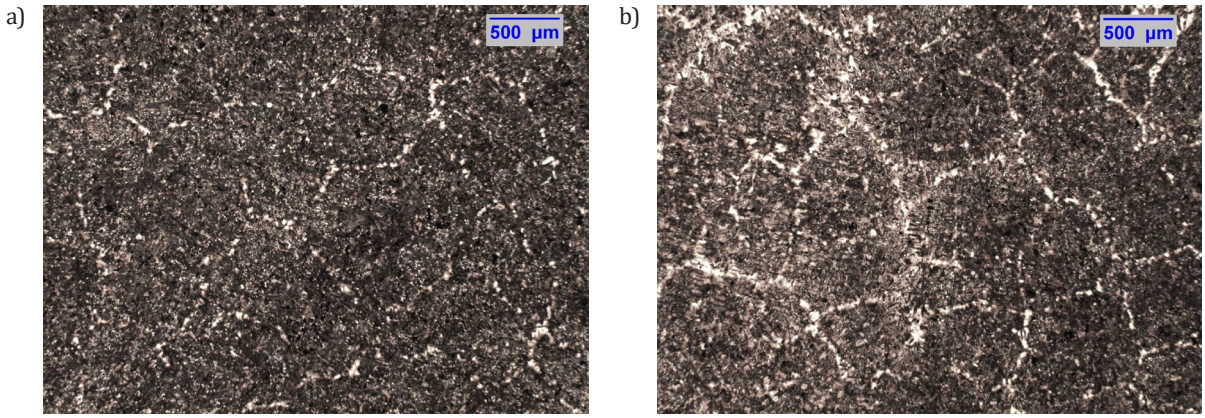

Fig. 14. Microstructure (area 5) of: a) Samples 3 and b) Sample 4 etched with Stead's reagent (magn. 25×)

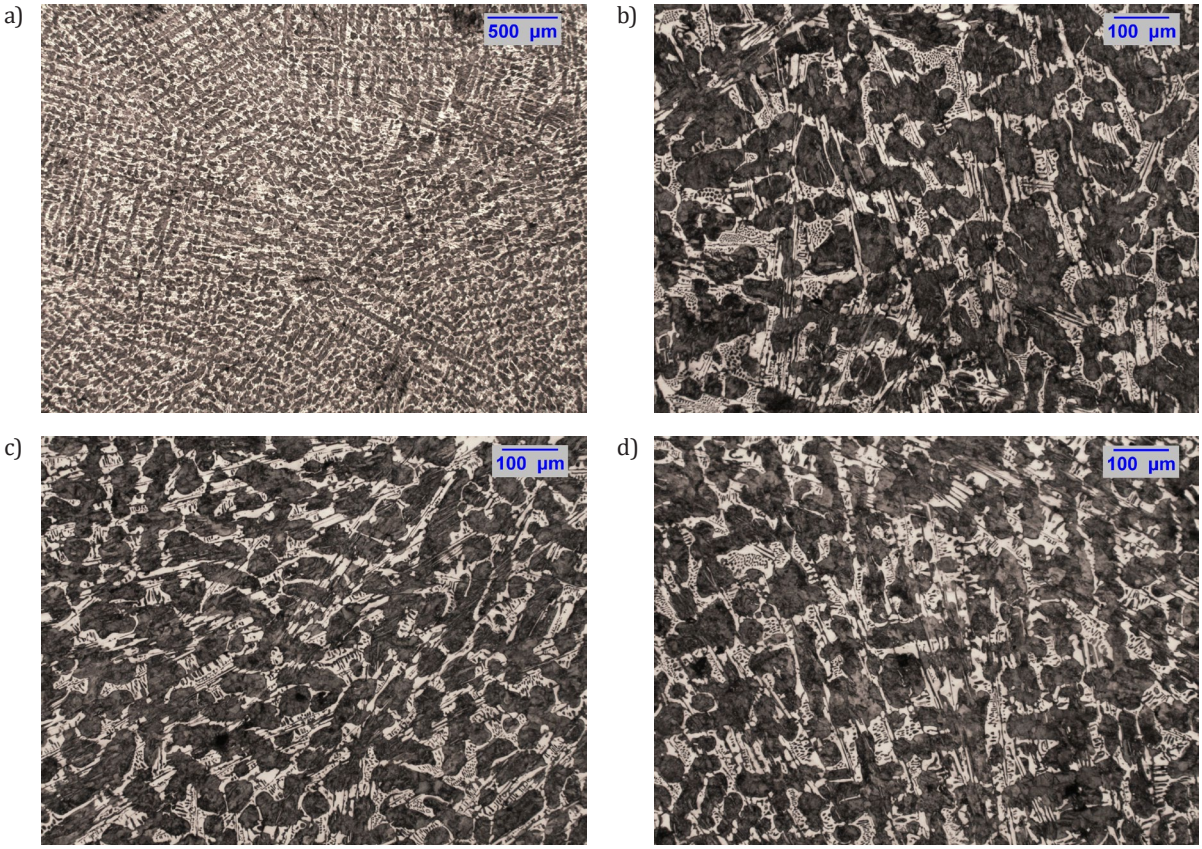

Fig. 15. Microstructure of Sample 5 etched with Nital: a) area 1, magn. 25×; b) area 2, magn. 100×; c) area 3, magn. 100×; d) area 4, magn. 100×

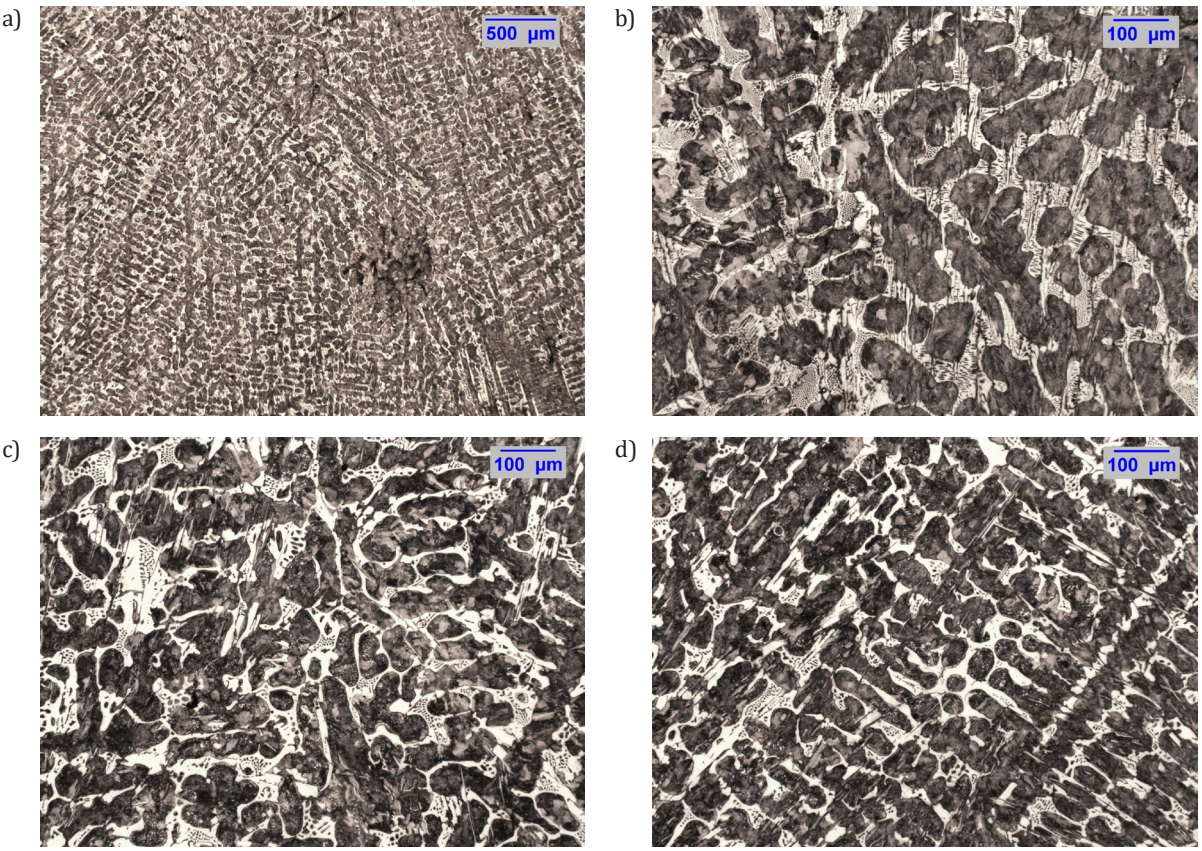

Fig. 16. Microstructure of Sample 6 etched with Nital: a) area 1, magn. 25×; b) area 2, magn. 100×; c) area 3, magn. 100×; d) area 4, magn. 100×

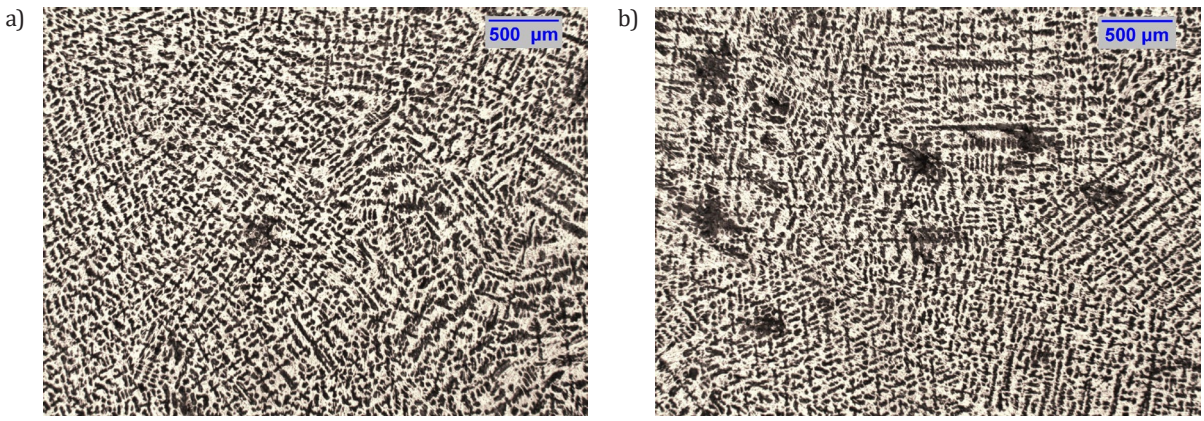

Fig. 17. Microstructure (area 5) of: a) Samples 5 and b) Sample 6 etched with Stead's reagent (magn. 25×)

The results of the quantitative metallographic analysis are presented in the Tables 1–4.

Table 1
Volume fraction of microstructure components in Samples 1 and 2

No. of Sample	Ledeburite [%]	Graphite [%]	Pearlite [%]	Ferrite [%]
Sample 1	25	13	62	0
Sample 2	28	19	53	0

Table 2
Volume fraction of microstructure components in Samples 3 and 4

No. of Sample	Ledeburite [%]	Graphite [%]	Pearlite [%]	Ferrite [%]
Sample 3	0	29	58	13
Sample 4	0	36	56	8

Table 3
Volume fraction of microstructure components in Samples 5 and 6

No. of Sample	Ledeburite [%]	Graphite [%]	Pearlite [%]	Ferrite [%]
Sample 5	23	3	74	0
Sample 6	18	5	77	0

Figures 10–17 show the microstructures of Samples 1 and 2, 3 and 4, and 5 and 6 etched with Nital and Stead's reagent.

Tables 1–3 present the volume fractions of the components of the microstructure in Samples 1 and 2 as well as 5 and 6. Table 4 gives data on the lengths of the four longest graphite precipitates in Samples 3 and 4.

In Samples 1 and 2 (Figs. 10–12), the microstructure of the white hypoeutectic cast iron was mainly detected. Separate "islands" of stable austenitic-graphite eutectics were found. Metal matrix has pearlite microstructure.

The microstructure of Samples 3 and 4 (Figs. 13–14) consists of a stable eutectic with a pearlite-ferritic base with a volume fraction of ferrite of not more than 13%. In these samples, there is small interdendritic Type D graphite (Sample 3–90%; Sample 4–80%), as well as Type E interdendritic graphite (Sample 3–10%; Sample 4–20%) according to PN-EN ISO 945-1: 2018-04. The number of eutectic grains per unit surface area of the sample is as follows: Sample 3–N_a = 180 mm^{-2}; Sample 4–N_a = 225 mm^{-2}.

Table 4
Results of measuring lengths of four longest graphite precipitates based on five micrographs [µm]

Sample 3 – Measuring areas 1–5						
No. Measurements	**1**	**2**	**3**	**4**	**5**	
1	87.4	97.5	144.2	165.1	137.3	
2	114.6	59.9	137.9	70.1	136.4	
3	101.8	65.5	99.7	82.8	87.5	
4	94.2	64.9	92.3	95.3	75.2	
Average value for sample	99.5	72.0	118.5	103.3	109.1	100.5
Sample 4 – Measuring areas 1–5						
No. Measurements	**1**	**2**	**3**	**4**	**5**	
1	51.3	148.9	108.6	67.5	79.3	
2	53.8	77.4	130.3	107.8	112.8	
3	57.8	75.9	71.2	54.5	87.8	
4	50.1	81.7	83.2	61.6	80.5	
Average value for sample	53.3	96.0	98.3	72.8	90.1	82.1

The microstructure of the ledeburite in the unalloyed iron as well as the clearly pronounced dendritic microstructure indicate that the iron has a hypoeutectic composition far from the eutectic point. This is noticeable in Samples 1, 2, 5, and 6; in Samples 5 and 6, the volume fraction of graphite is much less than in Samples 1 and 2. Effective modification prevented chill in the gray cast iron matrix.

In Samples 3 and 4, interdendritic graphite of Types D and E is present. Such precipitations of graphite are usually observed in strongly hypoeutectic cast iron or in the case of a weak modification. A more effective modification can lead to a decrease in the volume fraction of Type D graphite and increase the fraction of the graphite emissions of Type A. The magnitude of the eutectic grain ($N_a \sim 200$ mm^{-2}) indicates the weak effect of modification.

The results of measuring the length of the graphite precipitates within one sample indicate a high dispersion of this parameter. The difference in the results between Samples 3 and 4 obtained from a single cast iron sample differs by 20–25%, with this criterion $\overline{Z}$ = 5.15 K. To assess the effectiveness of modifying the cast iron considering the strong correlation, the best estimate is to determine the number of grains.

As a whole, it is established that the curves with numbers 1–2, 3–4, and 5–6 are similar to each other pairwise. This is clearly displayed in the criteria for recognizing of the cooling curves (Fig. 9). As we see, the $\overline{Z}$ criterion reacts sensitively to the slightest changes in the chemical composition and structure of the samples.

4. CONCLUSIONS

1. An advanced computerized method of derivative thermal express-analysis (TDA) of cast iron melts for the quality control of metallurgical processing and the complex of casting properties has been developed.
2. The errors of the method have been determined taking into account Student's criterion, and the high sensitivity of the method to the metallurgical history of the melts of cast iron has been confirmed.
3. The method has been successfully tested under laboratory and experimental-industrial conditions on castings of induction smelting.
4. The new method uses disposable environmentally safe steel thin-walled samplers of immersion with heat-resistant coating from inside and outside.
5. The method allows us to quickly adapt to the conditions of specific foundry shops and sections (especially with the frequent changing of the types of cast iron) due to the replenishment of the reference sample database.
6. The developed TDA method reliably provides the express-control quality of the melt quality of cast iron and finite cast iron castings.

The quality control of melted iron using the $\overline{Z}$ criterion is relevant due to the fact that this method with a high accuracy can prevents obtaining of the mottled structure of casting instead of gray one, if the melt quality is not optimal. This kind of the defects is one of the most frequent and most expensive types of rejects of gray iron castings in the real foundry industry.

Information about the microstructure of castings at room temperature in digitized form is in the database of the corresponding reference curve. The search for a suitable reference curve is performed using the similarity criterion. The thermal curve of a sample under study is recorded using the algorithm described in detail in the text of the article.

The actual data obtained by the TDA express method are used to monitor online to analyze the quality of a melt using a complex of microstructure indicators at room temperatures. If the microstructure meets the requirements of the relevant standards and/or agreed terms of the supply contract, then the command is given to fill the molds.

If the microstructure of the cast iron is unsatisfactory, the casting of the casting molds is immediately terminated in order to carry out the corrective processing of the melt in a smelting furnace or ladle. Corrective processing is implemented in the form of a technological operation of modification or modification along with inoculation. The processing method is determined by the type of the actual microstructure obtained by the express TDA method. The decision is independently made by the technologist or master of a casting site at his own responsibility based on past experience or by using an automated computer advisor.

Acknowledgements

The work is carried out in the framework of a Ukrainian-Polish joint research project under the agreement on scientific cooperation between the Polish Academy of Science and the National Academy of Science of Ukraine No. 51 "Development and verification of the innovation system of forecasting the quality of iron castings from derivative thermal analysis of the melt."

REFERENCES

[1] Binczyk F. (2007). An Assessment of the Derivative Thermal Analysis of Gray Cast Iron. *Archives of Foundry Engineering*, 7(3), 21–24.
[2] Li Y., Hu X. & Xu X. (2001). Pattern Recognition on Thermal Analysis. *Journal of Materials Science & Technology*, 17(1), 73–74.
[3] Pustyl'nik Ye.I. (1968). *Statisticheskiye metody analiza i obrabotki nablyudeniy.* Moskva: Nauka [Пустыльник Е.И. (1968). *Статистические методы анализа и обработки наблюдений.* Москва: Наука].
[4] Li Y. & Wang Q. (2005). Intelligent evaluation of melt iron quality by pattern recognition of thermal analysis cooling curves. *Journal of Materials Processing Technology*, 161, 430–434.
[5] Wang Q., Li Y.X. & Li X.C. (2003). Grain Refinement of Al-Si Alloys and the Efficiency Assessment by Recognition of Cooling Curves. *Metallurgical and Materials Transactions A*, May, 1175–1182.
[6] Li D.-Y., Xu Z.-Y., Ma X.-L. & Shi D.-Y. (2015). Review of current research and application of ductile cast iron quality monitoring technologies in Chinese foundry industry. *China Foundry*, 12 (N4), 239–249.
[7] Dawson S. & Popelar P. (2013). Thermal Analysis and Process Control for Compacted Graphite Iron and Ductile Iron. Keith Millis Symposium on Ductile Cast Iron: Oct. 15–17 2013. Nashville, TN, US. Red Hook: Curran Associates, 59–66.

[8] Dawson S. (2002). Process Control for the Production of Compacted Graphite Iron. Based on a presentation made at the 106th AFS Casting Congress. Kansas City: May 4–7 2002, http://www.cintercast.com, 1–11.

[9] Zakharchenko E.V., Zhukov L.F., Sirenko Ye.A., Bogdan A.V., Goncharov A.L., Kravchenko Ye.V. (2015). Usovershenstvovaniye universal'nogo metoda termicheskogo ekspress-analiza zhidkikh chugunov, osnovannogo na raspoznavanii formy krivykh okhlazhdeniya. *Protsessy lit'ya*, 2, 3–9 [Захарченко Э.В., Жуков Л.Ф., Сиренко Е.А., Богдан А.В., Гончаров А.Л., Кравченко Е.В. (2015). Усовершенствование универсального метода термического экспресс-анализа жидких чугунов, основанного на распознавании формы кривых охлаждения. *Процессы литья,* 2, 3–9].

[10] Zakharchenko E.V., Sirenko K.A., Goncharov A.L. & Bogdan A.V. (2015). Pat. Ukraine N99968.

[11] Sun Y.Z., An G.Y. (1995). The influence of structure parameters of cast iron sample cup on shape of cooling curve. *Research Studies on Foundry Equipment*, April, 35–38.

[12] Sun Y.Z. & An G.Y. (1995). The influence of structure parameters of cast iron sample on carbon equivalent. *China Foundry Machinery and Technology*, February, 48–50.

[13] Sun Y.Z., Che S.X. & Chen H.S. (1995). The influence of structure parameters of sampling cup on the precision of forecasting silicon content of cast iron. *Foundry Technology*, March, 6–8.

Journal of Casting & Materials Engineering Vol. 3 No. 2 (2019) 43–49
http://dx.doi.org/10.7494/jcme.2019.3.2.43

Recycling of Dispersed Metal Wastes in Rotary Furnaces

Sergei Leonid Rovin[a*], Alexander Sergei Kalinichenko[b], Leonid Efim Rovin[c]

[a] UE "Technolit", Ya. Kolasa Str., 24, Minsk, 220013, Republic of Belarus
[b] Belarusian National Technical University, Nezavisimosty Ave. 65, Minsk, 220013, Republic of Belarus
[c] Sukhoi State Technical University of Gomel, Prospect Octiabria 48, Gomel, 246746, Republic of Belarus
**e-mail: technolit@tut.by*

Received: 13 May 2019/Accepted: 11 July 2019/Published online: 31 July 2019

Abstract

The recycling of dispersed metal containing wastes is a considerable problem, as their accumulation in dumps today is commensurate with the volume of ore extraction. Several methods and technologies are developed to recycle metal containing wastes but almost all of them require the preliminary preparation of wastes resulting in an increased price of the recycled metals. Furthermore, it is especially difficult to recycle dispersed multicomponent wastes and, therefore, the problem of developing effective, flexible and reliable technology for recycling of dispersed metal containing wastes is still a pressing one.
The article presents an alternative method of recycling dispersed iron-containing wastes based on a continuous solid-liquid process of iron oxides reduction in rotary tilting furnaces (RTF). The new method allows the processing of waste of almost any composition and state: from metal lumps to oxide and multicomponent (chips, scale, sludge, etc.) wastes, contaminated with moisture, oils, organic impurities without their preliminary preparation (cleaning, homogenization, pelletizing, etc.). The result of recycling is the production of cast iron or steel ingots or required casting alloys. Some features of technology are considered, including the gas flow and motion of charge metal particles within the RTF. Process parameters providing high metal output are established.

Keywords:

recycling, dispersed metal wastes, rotary tilting furnaces, heat and mass exchange, mix, reduction

1. INTRODUCTION

In conditions of a growing shortage of high-quality charge materials and their rising prices, the recycling of dispersed iron-containing wastes (chips, scale, aspiration and abrasive dust, sludge, etc.) has become particularly important as their accumulation in dumps today is commensurate with the volume of ore extraction, and poses a serious environmental threat [1].

Traditional melting units in foundries and metallurgical plants are not adapted to the melting of dispersed materials. Therefore, almost all well-known recycling technologies of dispersed metal waste require their preliminary agglomeration (briquetting, balling etc.). However, briquetting of even the most valuable part of these wastes (steel and cast iron chips) does not allow charging material to be obtained that meets the quality of dense lump scrap [2, 3].

Before processing, metal wastes undergo multistage preliminary preparation, the cost of which reaches 60–80% of the resulting metal cost. A new concept of recycling is based on a flexible low-tonnage technology and equipment that allows cost-effective processing of relatively small amounts of heterogeneous waste in their initial state without preparation and pelletizing, resulting in the production of high-quality charge materials or alloys. The implementation of this process is carried out by means of rotary tilting furnaces (RTF) with a controlled gas flow vector and an inclined axis of rotation, providing higher heating rate and lower dust losses compared to traditional direct-flow drum furnaces [4, 5].

The developed technology is based on the intensification of physical and chemical processes due to the processing of individual particles of the material with a characteristic particle size of not more than 1–3 mm and typified by a developed reaction surface and porosity. These features allow a tenfold increase in the rate of heating, recovery and melting processes [4].

The study of the properties of dispersed metal waste, the study of solid- and liquid-phase reduction processes, operating and design characteristics of rotary furnaces using simulation and computer simulation, field experiments allowed the development of the theoretical and technological basis of flexible, cost-effective, low-tonnage recycling and introducing it into production. This opens up the possibility for foundry shops and machine works to create their own raw material base for foundry production. Moreover, it is possible to organize a waste-free system of metal turnover in machine-building enterprises.

2. FEATURES OF DISPERSED MATERIAL MOTION AND GAS FLOW IN THE RTF

More than 60% of all technogenic metal wastes are dispersed materials: shavings, slag, sludge, abrasive and aspiration dust etc. Lumps of dense scrap have long been used as a valuable charging material and processing them is not difficult. The situation with the remelting of dispersed metal wastes, particularly the oxide and multi-components ones, is rather different as to date no technology has been developed to the proper degree. Losses are up to 50% in cupolas or electric furnaces when melting dispersed materials (even the most valuable part of such waste – chips) run without their preliminary preparation due to entrainment and fumes. Cold briquetting of chips does not allow high-quality charge materials to be obtained. Better quality briquettes are obtained by pre-cleaning, sorting, adding binders and reductants with further high-temperature heating and pressing under high specific pressure. But even in this case the briquettes do not correspond to the quality of dense lump scrap despite often costing more to produce

It is known that a significant acceleration of heat and mass transfer processes, including transfer of gaseous reducing agents CO and H_2 deep into the particles, can have an impact. As a result, the role of direct reduction during the treatment of dispersed porous materials becomes stronger due to the increase of the reaction surface. To realize this effect, it is necessary to purge the layer of dispersed particles with a gas – heat carrier-reducing agent. It can be done in installations with a "boiling layer" or in a pneumatic stream for mono-dispersed material. For poly-dispersed metal waste, effective mass transfer can only be arranged by mixing the material itself, and this can be achieved most easily in rotating drum units (so-called short-drum furnaces are used for melting). However, there are restrictions in straight-through furnaces on the speed of the gas-heat carrier motion which cannot exceed the flying speed of heated material's particles (usually 3–5 m/s), which does not allow a high heat transfer coefficient to be obtained $\alpha = f(\mathrm{Re}, \mathrm{Nu}, \mathrm{Pr})$, where Re, Nu, Pr are Reynolds, Nusselt and Prandtl criterial numbers respectively. As a result, such furnaces are characterized by low thermal efficiency (not more than 10–15%) [5]. To increase the thermal efficiency of the rotary furnace there is a trend to make an increased length (to 40–160 m or more, e.g. tubular furnace). The heat balance is improved, but it is impossible to melt wastes in such furnaces as the process becomes poorly controlled.

Recently introduced rotary tilting furnaces with loop-like gas movement open up new possibilities in the processing of dispersed materials (Fig. 1).

The motion study of non-isothermal flow of gases in the RTF, the temperature fields and the intensity of heat exchange performed on full-scale units and by computer simulation allowed us to determine that the movement of gases in such furnaces has a complex circulation in nature. The speed of rotation is significantly higher (5–8 times) than the translational speed of the flow, resulting in increases in gas residence time in the working space and higher efficiency of heat transfer. Moreover, losses of dispersed and ultradispersed particles become lower [6].

The study of the gas flows was performed by applying a 3D-model of the furnace created in SolidWorks 14.0 and divided by ANSYS Meshing into a grid with the number of elements equal to 290,665. The results of numerical simulation are temperature fields, velocity and trajectory of the gas flow. Examples of the results obtained are shown in Figure 2 [6].

The aerodynamics of the flow and its interaction with the material depends on the location of the burners, their number and angle of attack as well as the layer configuration. The direction of rotation can be changed under certain conditions.

A simulation technique to study the nature and features of dispersed materials movement in the RTF was developed. The model was realized on the basis of hydrodynamic similarity principles. It was found that the dispersed materials in the RTF make a helical reciprocating motion which provides active mixing of the dispersed material both in the radial and axial direction.

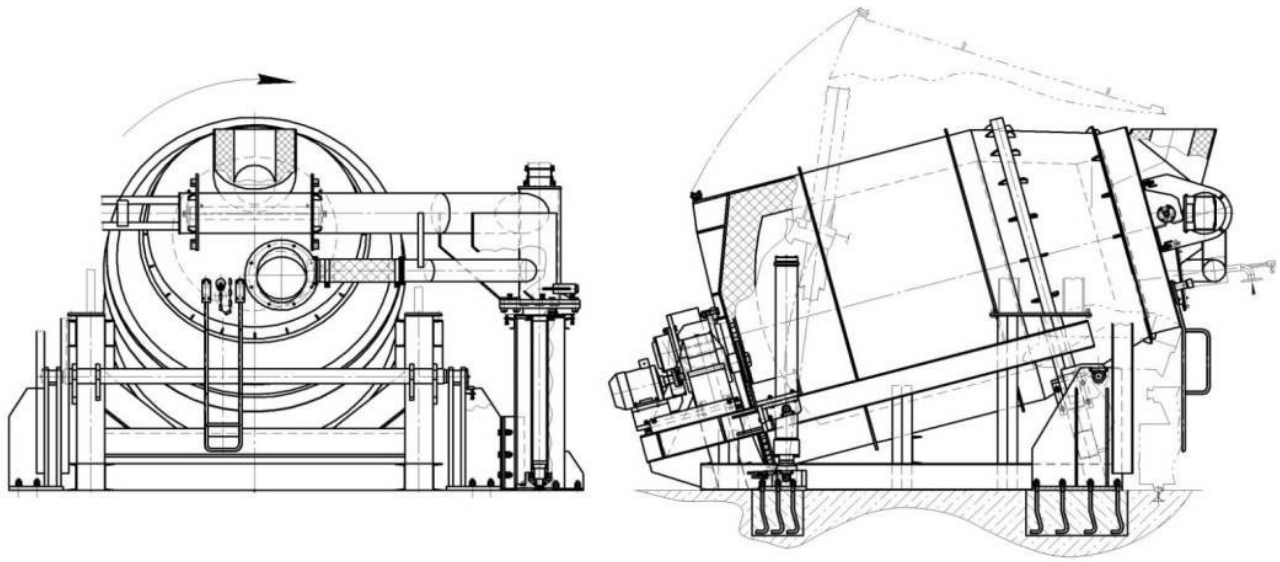

Fig. 1. General view of the RTF with loop-like movement of gases developed by UE "Technolit"

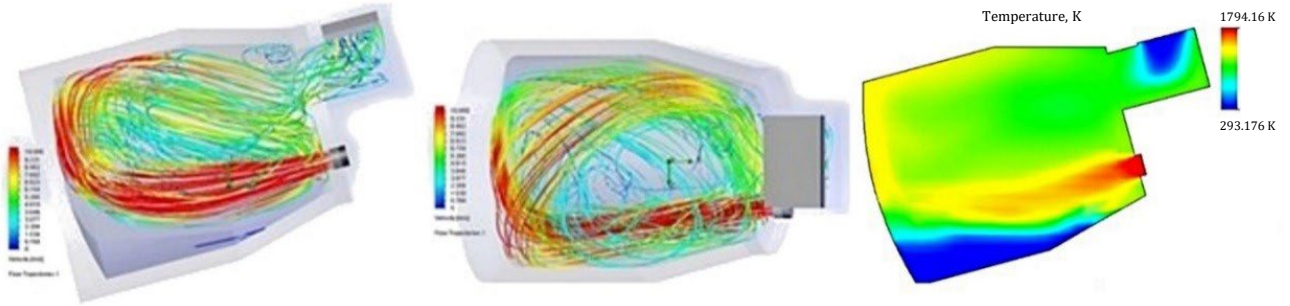

Fig. 2. The trajectory and velocity of gas movement as well as temperature fields in the RTF

The speed of material's "rotation" in the cross section exceeds the rotation speed of the furnace by 2–3 times and depends on the adhesion and autoadhesion properties of the material and the relative volume of the furnace charge.

Computer simulations were carried out using software CD-Adapco Star CCM+, Prometech Particle Work and the method of discrete (finite) elements DEM (Discrete Element Method) to determine the quantitative characteristics of the movement both the layer and individual particles of the material in the RTF. These data are necessary to obtain the real parameters of heat and mass transfer for further calculation and the design of furnaces. The calculations were performed on the basis of the instantaneous balance of gravity, inertia and contact forces of the particles considered with other particles and the furnace surface. The particles are considered as solid and elastic bodies and their size is determined by the data of field experiments, taking into account the scale factor. The particles undergo translational and rotational motion. Calculations take into account also the forces of adhesion and autoadhesion [7–9]. As a result of the numerical simulation, data about the nature of the dispersed materials movement in rotary furnaces with an inclined axis of rotation, the layer structure, trajectories and velocities of individual particles were obtained for the first time. The mixing process in the dynamic layer was investigated as well.

The velocities of the particles in the center and on the periphery of the layer may differ by tens or even hundreds of times, but there is no clear boundary between the zones. In addition, the absolute values and the velocity distribution vary over time and depending on the distance of the cross section relative to the bottom or neck of the furnace. Aerodynamic forces of high-speed gas flow affect the top layer of particles, especially in the collapse. In the cross section, the dynamic layer becomes lentil-shaped. Some results of the modeling of the material motion in the RNP are shown in Figures 3–5 [10].

In accordance with the fact that the heat transfer by convection occurs under conditions of macro-volumes mixing, the obtained data on the mixing velocities in the RTF allow us to calculate the volumetric heat transfer coefficient in the layer (α_v).

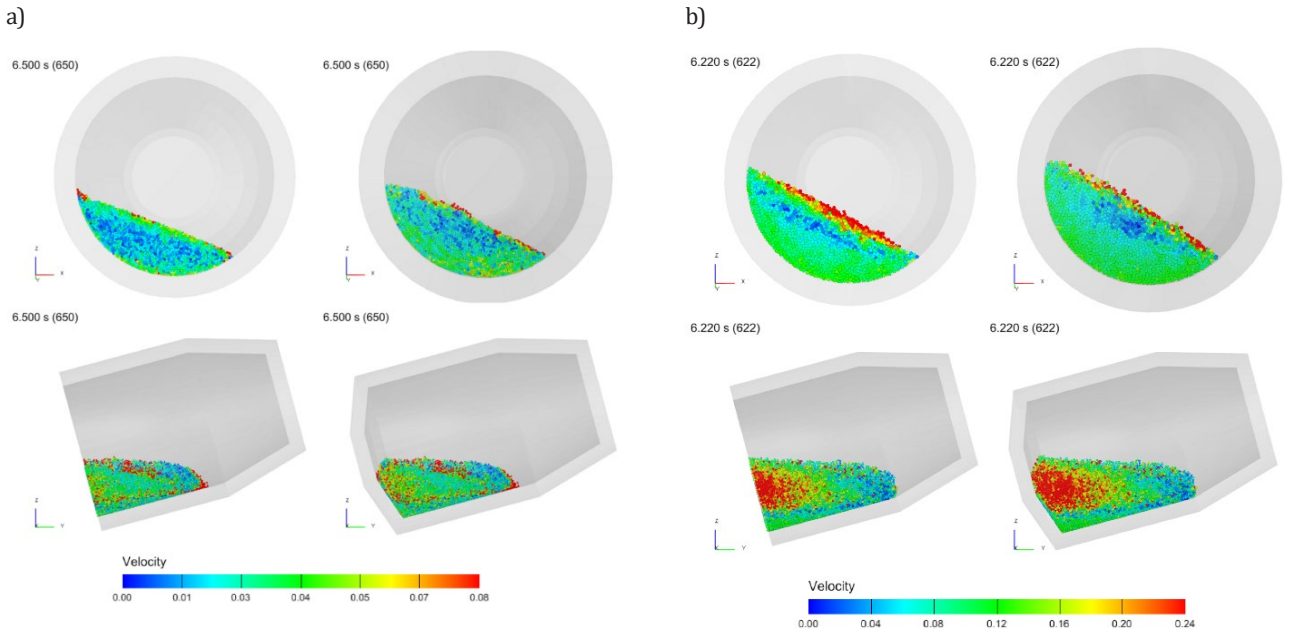

Fig. 3. The distribution of dispersed particles velocities in the layer of material in the RTF: a) rotation of the furnace at a speed of 5 rpm; b) rotation of the furnace at a speed of 10 rpm

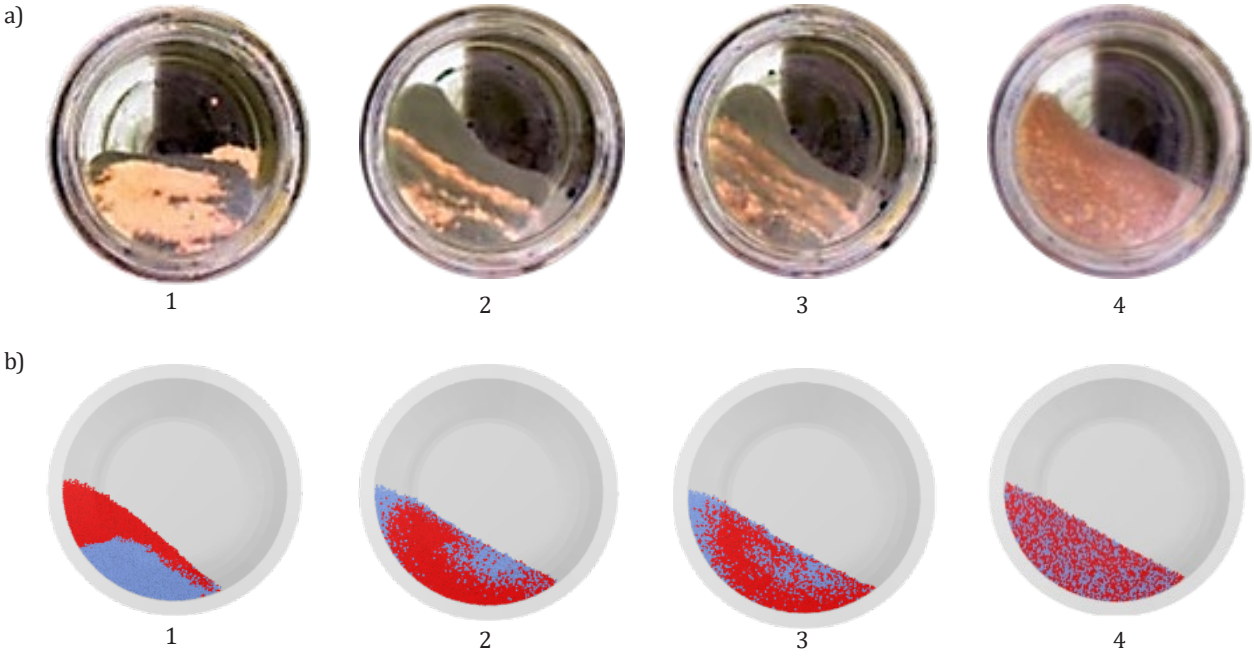

Fig. 4. Mixing of the material in the RTF: a) simulation modeling; b) computer simulation: 1 – the beginning of the rotation; 2 – one revolution of the housing; 3 – two turns; 4 – six turns

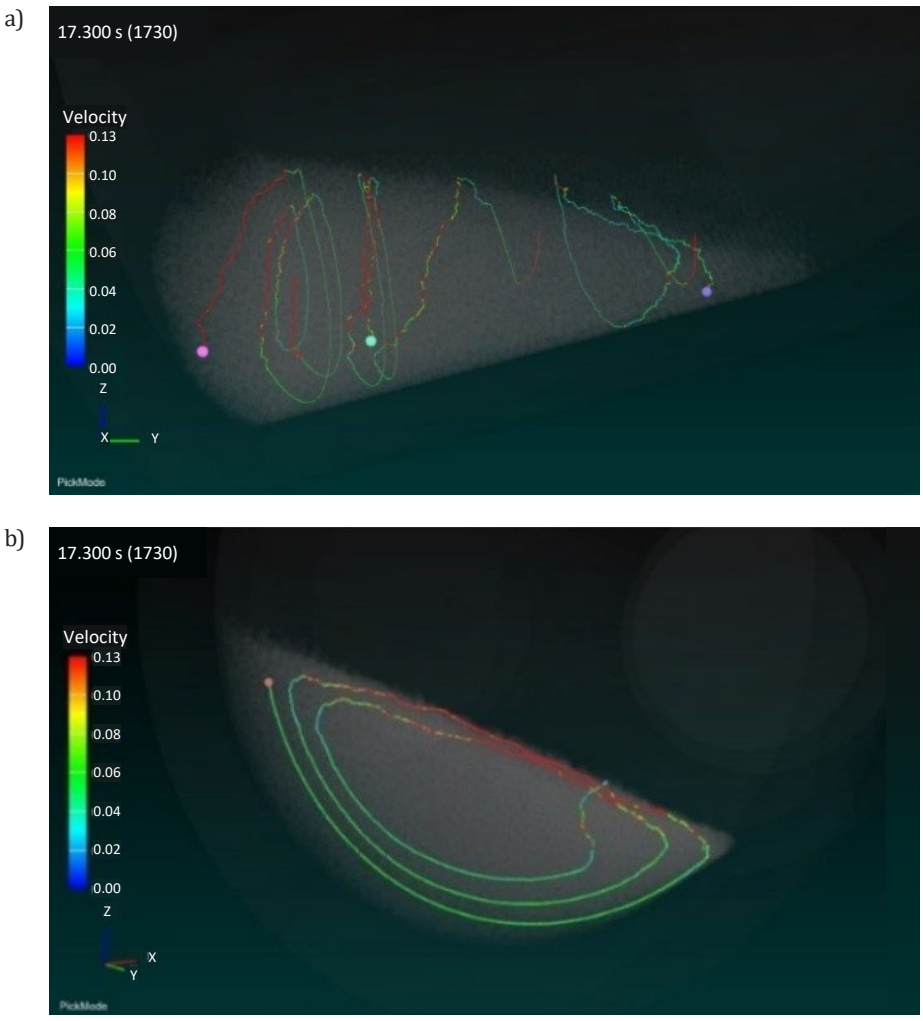

Fig. 5. The trajectory of the dispersed material particles in the RTF: a) longitudinal direction; b) cross-section

The heat balance, taking into account the heat loss with the exhaust gases, determines the heat consumption for heating the material to a predetermined temperature and at the same time the heat energy consumption by the heat carrier gas.

The calculated values for the experimental conditions (for the stirred blown layer) are α_v = 2750–3100 W/m^3, which are almost 3 orders of magnitude higher in comparison to the heating of the stationary layer.

The results of the simulation and numerical simulation of gases and dispersed materials motion under non-stationary conditions served as the basis for the development of technical solutions aiming at the intensification of rotary furnaces. Rotating tilting furnaces of different design and with controlled gas flow vector have been successfully implemented in practice. The created units allow working effectively with dispersed waste of both ferrous and non-ferrous metals. The efficiency of furnaces reaches 50–55%, which is 3–5 times higher compared to electric induction, arc or stationary fuel furnaces when working on such materials.

The obtained results on the processes of movement and mixing of dispersed materials can also be used for the calculation and modernization of mixers for various purposes, painting chambers, cladding installations and other rotating type units.

3. HEATING AND REDUCTION OF DISPERSED MATERIALS IN RTF

Unlike traditional installations, working with a fixed layer of lump materials, in the RTF material makes a continuous helical reciprocating motion, actively mixing, and constantly interacting with a high-speed turbulent gas flow, making a loop-like motion in the working space of the furnace [6].

Constant updating (mixing) of the layer and its intensive purging greatly accelerate the heat transfer processes. The small particle size of the material layer (from $3\cdot10^{-2}$ to $1\cdot10^{-4}$ m) as well as the porosity and microporosity of oxide particles (up to 0.05–1.0 μm) make the main contribution in high intensity of the heating process. Accordingly, the area of the reaction surface of a dispersed particles layer (e.g. scale) is 0.5–2.5 m^2/g.

Heating the chips or forging scale to a temperature of 750–850°C in the industrial RTF with a capacity of 2–4 tons took 15–18 minutes using a natural gas burner with a capacity of 1.0 MW. Natural gas consumption ranged from 11 to 14 m^3/t for clean dry charge and 8–10 m^3/t for heating the chips contaminated with oils. Heating of iron-containing materials must be carried out at high speed and in an oxidation-free atmosphere. Dispersed wastes containing carbon (coke, coal, lignin) are loaded into the furnace, providing the formation of an oxidation-free atmosphere. Basically high temperature oxidation-free heating of the chip is commonly applied in a duplex process RTF-induction crucible furnace. This process allows a reduction of electricity consumption for 180–220 kW·h/t and up to 30–35% of the melting time.

The recycling of oxide iron containing materials is a more difficult and complicated process. The reduction of oxides is almost impossible in traditional melting furnaces of foundry shops (cupolas, induction and arc furnaces). It is proved by half a century of unsuccessful experiments with the organization of reduction cupola melting with the help of composite briquettes containing various reducing agents [3]. In contrast to the above mentioned furnaces, the RTF allows the entire cycle of oxide metal waste processing to be carried out consistently: drying, removal of contaminants, heating, pre-reduction in the solid phase and then rapid transfer of the material into the liquid phase, the final liquid phase reduction and refinement of the melt to a given composition (grade). The recovery effect reaches a level close to a theoretically possible one. As a result, both steel and cast iron can be obtained from iron-containing waste. This is a tremendous advantage of the technology developed compared to usual metallurgy, where the process ends at the stage of sponge iron: metallized pellets or briquettes. In RTF, reaction surface increases and the speed of heating, reduction and melting processes increases tenfold. The "Quasi-homogeneous" model of the reduction process can adequately describe the physical-chemical processes of dispersed porous materials reduction (scale, aspiration dust or metallurgical slurries). The model is based on the idea that the reducing agent penetrates and interacts with oxides throughout the cross section of particles. The speed of the process is the same and metallization occurs throughout the volume of the particles (layer element) at the same time. The degree of metallization reaches 75–80% after 30 minutes for reducing scale in a dynamic layer at a temperature of 1100–1200°C [4, 6].

The recycling process in the RTF is carried out as follows. The initial charge (iron-containing waste, reducing agent and fluxes) is loaded into the furnace filling 28–30% of the working volume without any preliminary preparation. Heating with gas or liquid fuel with a specific flow rate of 12–15 m^3/t is carried out when the furnace rotates at a speed of 3–5 rpm. When the temperature reaches 1000–1100°C charge is maintained for 1.5–2.0 hours (depending on the mass of the material) for the solid-phase reduction stage. At the same time, the furnace maintains a reducing atmosphere: CO/CO_2 = 1.5–2.5. At the end of the period there are small spherical granules of sponge iron. The degree of Fe reduction reaches 80–85%. Then, fluxes, reducing agent and additives are additionally loaded into the furnace and oxygen is supplied resulting in a temperature increase in the working space to 1700–1800°C. The rotation speed decreases to 0.5–1.0 rpm. Within 5–6 minutes, the process is moved to the stage of liquid-phase reduction (LPR), virtually bypassing the stage of screaming recovery. The duration of the LPR stage does not exceed 20–30 minutes depending on the requirements for the liquid metal, primarily to the carbon concentration in it. Then the metal is exposed until the end of the bale and merged into molds or ladle for secondary treatment. The flow rate of the reducing agent is within 40% of the mass of oxides (depending on their composition). Consumption of gas fuel is 120–130 m^3 per ton of scale and oxygen 25–30 m^3/t. Resulting iron-carbon alloys depending on the liquid phase reduction mode can be treated to a given composition and quality of branded alloys (cast iron and steel) [11]. However, more rational

is the use of RTF to produce high-quality charge material (ingots, pigs) for the subsequent smelting of branded alloys in traditional furnaces. For machine-building enterprises it is more attractively the organization of a duplex process, in which the metal obtained in RTF directly in liquid form is transferred to traditional electric smelting units or mixer to obtain the required chemical composition and exposition at a given temperature [4, 12].

During the reduction melting of scale and sludge, the duration of the SPR-process did not exceed 2.0–2.5 hours, and the entire cycle, including liquid–phase recovery to 95–99% and treatment to a predetermined composition was no more than 3–3.5 hours.

The technological intervals of obtaining iron-carbon alloys in the RTF in comparison with the known processes of iron direct reduction are shown in Figure 6.

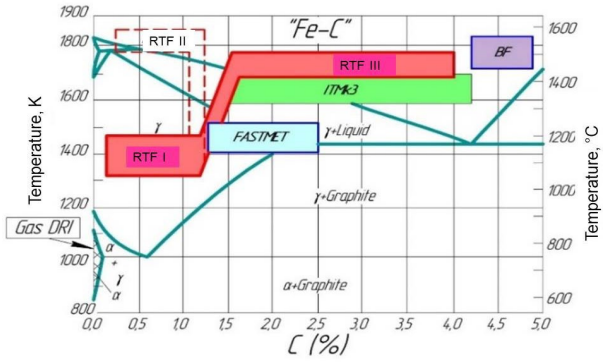

Fig. 6. Technological intervals of production of iron-carbon alloys in RTF

The process can also be used for recycling non-ferrous alloys, which has been verified by full-scale tests and subsequent implementation in the processing of lead, aluminum and copper alloys. Figure 7 shows examples of RTF for the recycling of a different dispersed metal wastes.

The developed technology and equipment, due to its technological flexibility, allows the use of waste of any composition, degree of contamination (including with oils and coolant), degree of oxidation (including scale and sludge), heterogeneity of properties and characteristics in a wide range of volumes starting from several hundred kilograms and up to two dozen tons in one charge, which ensures good adaptation to the conditions of existing production and does not require large investments in development.

The profitability of production shops in machine-building enterprises for processing their own dispersed metal waste is not less than 50%, and the return on investment is no more than 9–12 months. The production capacity of such shops can range from 0.5–1.0 thousand to 50–100 thousand tons of metal waste processed annually.

4. SUMMARY

The new concept of recycling based on flexible low-tonnage technology and special equipment allows cost-effective processing of relatively small amounts of heterogeneous waste in the initial state without preliminary preparation and pelletizing aimed at obtaining high-quality charge materials or alloys for foundries. The developed technology is based on the characteristic features of physical and chemical process-es and heat-mass transfer in the transition to the processing of material particles with a characteristic particle size of not more than 1–3 mm which are characterized with a developed reaction surface and porosity. As a result, it allows the speed of heating, reduction and melting processes to be increased tenfold.

Implementation of the technology is carried out applying rotary tilting furnaces with an inclined axis of rotation and controlled gas flow vector. Studies of the movement of non-isothermal gases flows and dispersed materials in the RTF, temperature fields and heat exchange intensity allowed the determination of the optimal design parameters of these furnaces and to develop recommendations for their design and operation.

The solution of the problem of ferrous and non-ferrous metals' dispersed wastes recycling opens up the possibility of the creation of one's own raw material base for a foundry. Moreover, it is possible to organize a waste-free system of metal turnover, improve the environmental situation and reduce the production costs of metal engineering and metalworking enterprises.

a) b) c)

Fig. 7. Rotary tilting furnace for the recycling of dispersed metal wastes manufactured by UE "Technolit": a) processing of cast iron shavings (GLS Tsentrolit, Gomel); b) recycling lead ("CPWR ALLOY", Ryazan, Russia); c) recycling of iron scale and sludge ("BMZ", Zhlobin)

REFERENCES

[1] *Recovering metals from waste.* Retrieved from: https://www.metso.com/industries/waste-recycling/waste-types/metals/ (accessed 17.08.2018).

[2] Valavin V., Makeev S., Pokhvisnev Yu., Zaytsev A. & Popov A. (2012). Recycling of Iron-Containing Waste of Metallurgical Works in the Countries of Black Sea Economic Cooperation (BSEC). *IX International Congress "Machines, Technologies, Materials",* 1, 79–81.

[3] Bogdandy L. & Engell H.-J. (2013). *The Reduction of Iron Ores – Scientific Basis and Technology.* Berlin: Springer/Link.

[4] Rovin S.L. (2015). *Retsikling metallootkhodov vrotatsionnykh pechakh.* Minsk: Belorusskiy Natsional'nyy Tekhnicheskiy Universitet [Ровин С.Л. (2015). *Рециклинг металлоотходов вротационных печах.* Минск: Белорусский Национальный Технический Университет].

[5] Schmitz C. (2003). *Handbook of Aluminium Recycling.* Essen: Vulkan-Verlag GmbH.

[6] Rovin S.L. (2016). Issledovaniye raboty rotatsionnykh naklonyayushchikhsya plavil'nykh pechey. *Nauka i Tekhnika*, 15(1), 18–28 [Ровин С.Л. (2016). Исследование работы ротационных наклоняющихся плавильных печей. *Наука и Техника*, 15(1), 18–28]. Doi:10.21122/2227-1031-2016-15-1-18-28.

[7] Warnatz J., Maas U. & Dibble R.W. (2006). *Combustion. Physical and Chemical Fundamentals, Modeling and Simulation, Experiments, Pollutant Formation.* Berlin: Springer-Verlag Berlin Heidelberg GmbH.

[8] Sonavane Y. & Specht E. (2008). Numerical analysis of the heat transfer in the wall of rotary kiln using finite element method ANSYS. *7th International Conference on CFD in the Minerals and Process Industries: December 9–11. Melbourne, Australia.* CSIRO, 1–5.

[9] Norouzi H.R., Zarghami R., Sotudeh-Gharebagh R. & Mostoufi N. (2016). *Coupled CFD-DEM modeling: formulation, implementation and application to multiphase flows.* Chichester: John Wiley & Sons.

[10] Rovin S.L., Rovin L.E., Zharanov V.A. & Mazurov V.S. (2017). Dvizheniye i smeshivaniye dispersnykh materialov vrotatsionnykh pechakh. *Lit'ye i metallurgiya,* 2, 117–127 [Ровин С.Л., Ровин Л.Е., Жаранов В.А. & Мазуров В.С. (2017). Движение и смешивание дисперсных материалов в ротационных печах. *Литье и металлургия.* 2, 117–127]. Doi:10.21122/1683-6065-2017-2-117-127.

[11] Rovin S.L. & Kalinichenko A.S. (2017). Primeneniye rotatsionnykh naklonyayushchikhsya pechey dlya organizatsii bezotkhodnogo oborota metallov na mashinostroitel'nykh predpriyatiyakh i proizvodstva otlivok. *ITB "Lit'ye Ukrainy".* 8 (204), 2–8 [Ровин С.Л. & Калиниченко А.С. (2017). Применение ротационных наклоняющихся печей для организации безотходного оборота металлов на машиностроительных предприятиях и производства отливок. *ИТБ "Литье Украины"*, 8 (204), 2–8].

[12] Negami T. (2000). Premium iron shot making by ITmk3. Commercializing new hot metal processes beyond the blast furnace. *Gorham conference proceeding. Atlanta, Georgia, USA,* 171–176.